Water Flux Across Lipid Membranes Observed by Variations in Electrical Capacitance

Alex Doermann
Brigham Young University
Applied Physics: Capstone Paper

Contents

Figures

Abstract

In this innovative and original technique, water flux across a lipid bilayer membrane is measured as a function of changing membrane capacitance. The capacitance of a lipid membrane can be directly measured with a high impedance amplifier as the current resulting from an applied $\frac{dV}{dt}$. The characteristic capacitance of a membrane is proportional to surface area. Since the membrane is fixed on a sealed pipette, a change in capacitance (surface area) implies a change in volume (e.g., bulging). The solution in the pipette will expand if heated, and thermal expansion of the solution will cause the membrane to bulge. Upon bulging to approximately 50-75% of its original (non-bulged) capacitance, a chemical gradient is added to the solution bath. The addition of a gradient induces osmosis, causing water to flow from the less concentrated pipette solution into the more concentrated solution bath. As water flows, the membrane resumes its normal, flat state, the change in capacitance can be found as a function of time. Using this data we can extrapolate the flux of water across the membrane.

Introduction

Fast communication in the human body is performed by neurons that conduct electrical impulses to and from the brain. Sensory neurons direct impulses to the brain conveying sensations such as sight and touch. The brain replies through motor neurons, which conduct impulses from the brain to voluntary skeletal muscles that move the body ("Neuron" 2012). As shown in Figure 1, Neurons communicate to other cells by releasing chemicals called neurotransmitters through the process of **exocytosis**. Before neurotransmitter can be released, it is packaged within synaptic vesicles inside the cell and released through a complex protein mechanism (Bock 2010). Vesicles are spherically shaped and surrounded by a lipid bilayer containing proteins (e.g., v-SNARE). The cell membrane has proteins (t-SNARE) that are complementary and specific for the v-SNARE proteins on the vesicle. The process of exocytosis is initiated when the v-SNARE proteins on the vesicle bind to the t-SNARE proteins on the cell membrane (Lang 2008). The role of **SNARE proteins** is to provide the energy required to pull the cell and vesicle membranes close enough together and initiate lipid rearrangement necessary for **fusion** (Wiederhold 2010); however, in vitro there are other mechanism that can be utilized to provide sufficient energy to drive vesicle fusion.

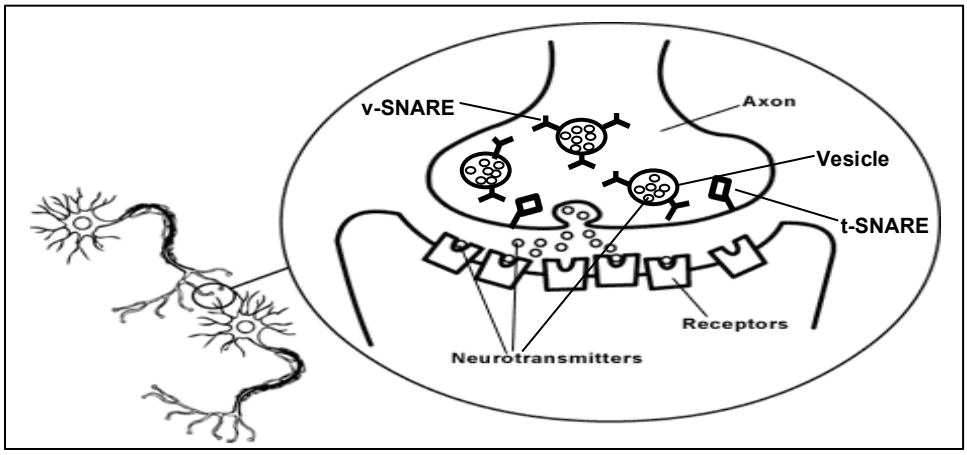

Figure 1: Cartoon showing the interaction between two nerve cells. Depicts vesicles

One method to initiate fusion without the SNARE complex is through a chemical gradient. Like the SNARE proteins, the addition of a chemical gradient helps overcome the energy barrier promoting fusion (Woodbury 1988). Upon addition of the gradient, fusion events begin being observed; simultaneously, water is constantly diffusing across the lipid bilayer, through osmosis, to the more concentrated solution. The flux of water through the membrane dictates the equilibration time between the two solutions. This is relevant to our lab because vesicle fusion ceases upon the equilibration of the two solutions.

Currently, we are measuring vesicle fusion to a membrane formed on a hole in a cup, but we want to measure fusions across a membrane on the end of a pipette. The orientation and surface area (capacitance) of a membrane have significant effects on vesicle fusion rates. On the cup, a vertical membrane is painted that has a low surface area; in comparison, on a pipette a horizontal membrane is painted with a higher surface area. Since the cup has a large volume, the equilibration time between solutions is long enough to collect an hour data set. A glass pipette only holds 5μL, so if the solutions equilibrate too quickly than this method is not a viable way to measure fusion events. If we find that the solutions equilibrate too fast then we will have to abandon the idea of vesicle fusion experiments with pipettes.

Measuring the water flux across lipid membranes has been a topic of study dating back forty years with Holz (Holz 1970). Holz used a more tedious method to measure the flux of water through crude and mixed lipid membranes. Later in 1995, Jansen measured the flux of water through several different lipids using a difficult and time extensive D_2O/H_2O experiment (Jansen 1995). These experiments have yielded results, but took extensive amounts of time and effort. A common modern technique in working with lipid bilayers is atomic force microscopy (AFM). AFM utilizes a "high-

resolution probe" that images objects on a nanometers scale. For imaging lipid bilayers, AFM requires stacked and supported lipid because of the frailty of the membrane (Reviakine 2000). In contrast to AFM, we use fully hydrated lipid bilayers in this study, which are similar to the bilayers found in the human body; thus, the experiments that are conducted more closely reflect the properties of lipid bilayers found in human cells. Modern technologies allow for us to attain these measurements through cleaner and simpler methods using electrophysiology.

Electrophysiology utilizes electrical properties, such as voltage and current, to quantitate certain properties of biological processes. Since a lipid membrane is composed of two layers of polar phosphate groups (heads) separated by non-polar alkyl groups (tails), it acts as parallel-plate capacitor. A parallel-plate's capacitance is proportional to surface area and inversely proportional to the distance between the plates. The charge that can be stored on a capacitor is defined by the characteristic capacitance of the capacitor and the applied voltage across the plates, i.e.

$$Q = C\,V.$$

By taking its time derivative we find that

$$\frac{dQ}{dt} \equiv I = C\,\frac{dV}{dt},$$

or

$$C = I/\frac{dV}{dt}.$$

Therefore, using electrophysiological approaches, the capacitance across a membrane can be measured by applying a known changing voltage and measuring the resultant current. By finding the capacitance of a membrane, the surface area of lipid membrane can be calculated (Bartlett 2008). Since capacitance is proportional to surface area, an increase in capacitance is correlated with an increase in

surface area; this increase in surface area is from the formation of a spherical cap (bulged membrane) with an enclosed volume (figure 2).

Therefore, by using geometry, algebra and calculus the capacitance and volume enclosed by a bulged membrane are closely correlated (Appendix A). In this study we measure the flux through a lipid membrane by measuring a change in capacitance. This technique is a novel and efficient way to find the flux through a membrane made of any desired lipid composition.

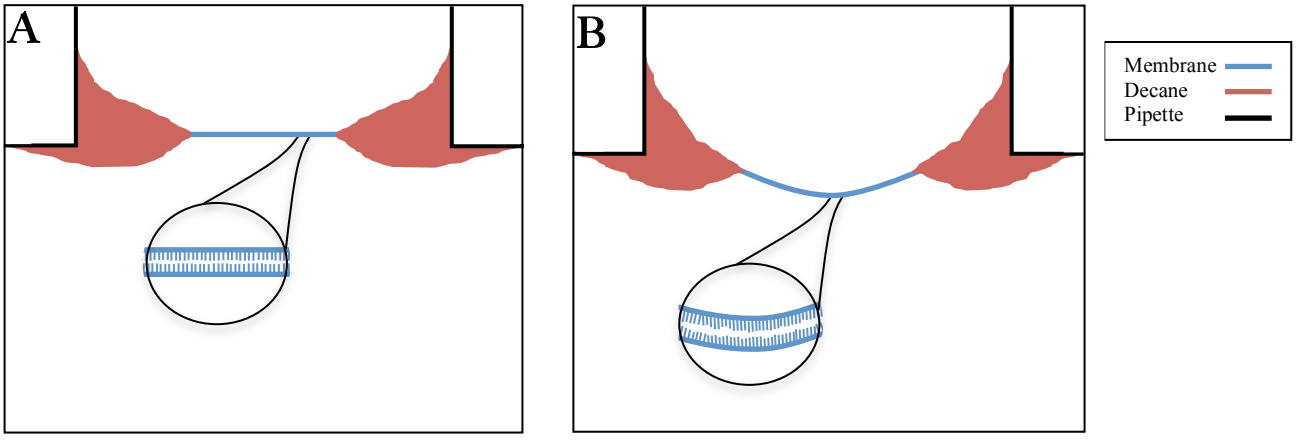

Figure 2: A. Cartoon depicting a membrane attached to a pipette. The decane torus (brown) results from dissolving lipids in decane and adds stability to the membrane. It also accounts for the difference in capacitance between the theoretical and actual capacitances. The blow up shows the bilayer in its initial unbulged state. **B.** Cartoon depicting the membrane in its bulged state. Note the decane retains the size from its unbulged picture in A. The only change is in the membrane size. The spherical cap produced contains a volume that allowed us to measure the flux out of the membrane.

Experimental Procedures

A 7:3 mixture of phosphatidylethanolamine (PE) and phosphatidylcholine (PC) lipids dissolved in chloroform are used for these experiments. We evaporate the chloroform from the solution using nitrogen gas. The pure PE: PC lipids are then dissolved with decane to make a 50 mg/ml solution. This lipid solution is painted over the tip of a submersed 5μL glass capillary pipette. The glass capillary

pipette is prepared by first pre-coating the pipette with lipids dissolved in decane. Since the lipids do not "stick" to glass very well, a pre-coat of decane and lipids allows a membrane to be painted more easily across the end of a capillary pipette (Tenchov 1989). Once the lipid pre-coat is dry (~5 minutes), the pipette is then filled with a KCl: HEPES buffer solution (150 mM KCl, 8 mM HEPES, pH 7.2) through **capillary action.** A silver chloride wire is inserted 2mm from pre-coated end of the capillary pipette while extending out the other end by about 10mm (figure 3A). While keeping the capillary pipette submersed in the buffer solution, the extended silver chloride wire is sealed to the glass using hot glue. Once the hot glue is set (~1 minute) and the wire is secure, the capillary pipette is removed from the solution and secured into an isolated chamber enclosed in a basic Faraday cage. In the isolated chamber, there is a liquid reservoir that is filled with about 4mL of KCl: HEPES buffer solution (figure 3B). The unsealed end of the capillary pipette is submersed about 2mm into the solution.

To get an electrical connection, both a wire extending out of the capillary pipette and an electrode that is in the reservoir are connected to a extremely sensitive amplifier (Warner Instruments® Model BC-535), measuring in the pA and pF ranges. A thermocouple is placed into the reservoir to measure the temperature of the solution in reservoir (figure 3B). Two stir bars are inserted into the

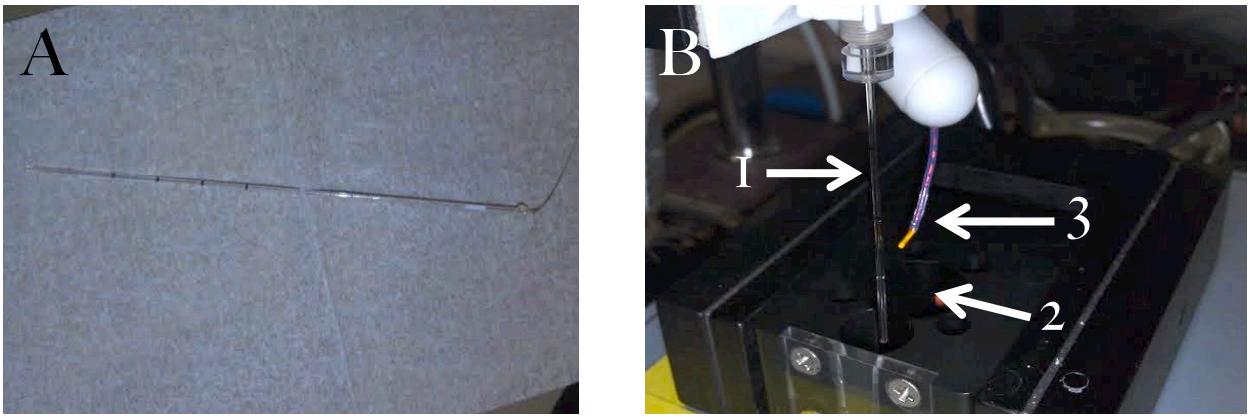

Figure 3: A. A 5µL capillary pipette that has a silver chloride wire inside it (the capillary pipette is 70mm long). **B.** The apparatus used to acquire our flux data. (1) The capillary pipette used in the capacitance experiment. (2)

chamber to avoid the possibility of introducing a temperature gradient into the solution. The stir bars and instrumentation is turned on allowing the system to equilibrate before painting a membrane on the pipette.

Upon equilibration of the system (~5 minutes, depending on the temperature), a membrane is painted on the submersed end of the pipette and the capacitance is checked across the membrane. Typically, the capacitance drifts for ~15-30 minutes as the membrane and decane torus form a stable interaction with the glass pipet. This process is sped up by exposing the membrane to a series of temperature oscillations that anneal the decane torus that surrounds the membrane (figure 2). The temperature of the solution is increased in chamber using a commercial peltier device (Warner Instruments' CL-100 Temperature Regulator®). The heat from the chamber slowly diffuses into the pipette causing the solution in the pipette to expand. Through the thermal expansion of water the membrane is bulged, increasing the measured capacitance.

Once the membrane has stabilized in it bulged condition, the stir bars are turned off and the chamber is opened. Quickly, a variable percent of the solution in the front chamber is exchanged with a 3M KCl solution to provide a concentration gradient. After putting the Faraday cage back over the system, about 5–7 seconds are needed to allow the amplifier to stabilize. The stir bars are then turned on to stimulate mixing of the gradient with the solution in the front chamber (figure 4). The water movement from the pipette into the solution bath is physically measured as the bulged membrane's capacitance decreases to its original capacitance. The flux is then found through analyzing the collected measurements using the following mathematical techniques.

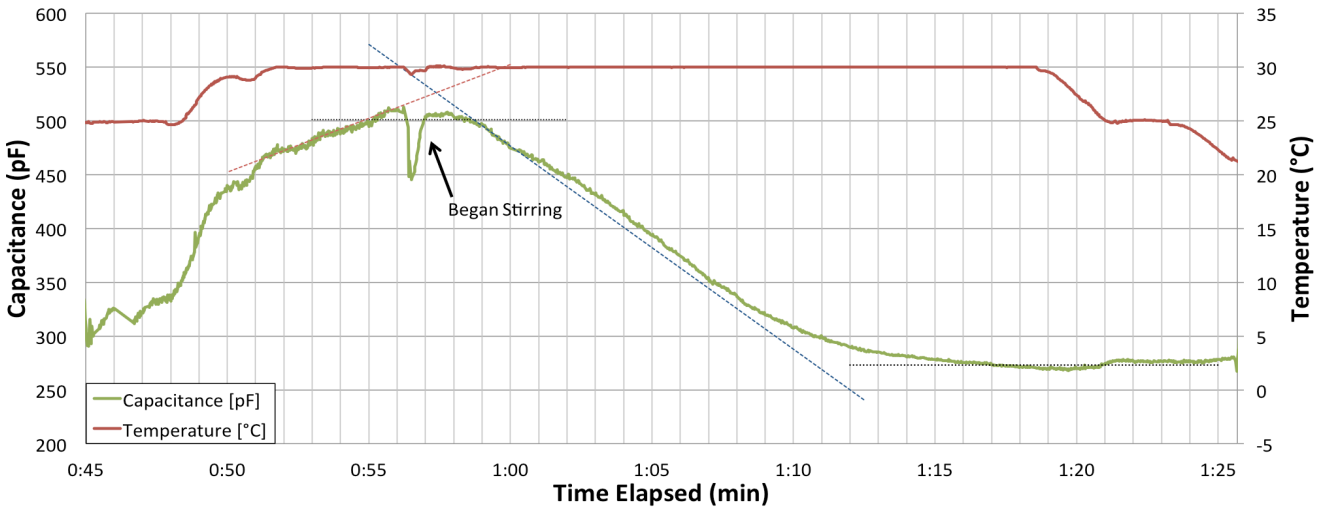

Figure 4: Data taken from a water flux experiment. The sharp decline in capacitance shows when we opened the box and added the gradient. The membrane was approaching 2x its original capacitance so we added a gradient before it equilibrated. In order to account for this, we added the positive slope from the bulging capacitance to decrease in capacitance induced by the gradient.

Theory

The areas of the membrane and decane can be found using the following technique:

$$A_p = \pi {r_p}^2,\ A_m^0 = \frac{C_0}{\mu},\ A_m^B = \frac{C_B}{\mu}, A_d = A_p - A_m^0,$$

where μ is the conversion constant for decane lipids, C_0 and C_B are the unbulged and bulged capacitances, r_p is the radius of the pipette, and A_p, A_m^0, A_m^B, and A_d are the areas of the pipette opening, the unbulged and bulged membrane, and the decane torus, respectively. Using geometry and algebra the height of the bulged membrane is calculated to be,

$$h = \sqrt{\frac{A_m^B - A_m^0}{\pi}} = \sqrt{\frac{C_B - C_0}{\mu\,\pi}}.$$

Knowing the height of the bulged membrane allows us to solve for the extra volume of solution capped by the membrane (Appendix A).

$$V(h) = \frac{\pi\, h}{6}\left(3{r_p}^2 + h^2\right),$$

$$V(C_B) = \frac{\pi\left(\sqrt{\frac{C_B - C_0}{\mu\,\pi}}\right)}{6}\left(3{r_p}^2 + \left(\sqrt{\frac{C_B - C_0}{\mu\,\pi}}\right)^2\right),$$

$$V(C_B) = \sqrt{\frac{\pi}{\mu}(C_B - C_0)}\left(\frac{{r_p}^2}{2} + \frac{1}{6\,\mu\,\pi}(C_B - C_0)\right),$$

$$V(C_B) = \sqrt{\frac{\pi}{\mu}}\left(\frac{{r_p}^2}{2}(C_B - C_0)^{\frac{1}{2}} + \frac{1}{6\,\mu\,\pi}(C_B - C_0)^{\frac{3}{2}}\right).$$

Through using the chain rule, we find:

$$\frac{dV}{dt} = \frac{dV}{dC_B}\frac{dC_B}{dt},$$

with

$$\frac{dV}{dC_B} = \sqrt{\frac{\pi}{\mu}}\left(\frac{{r_p}^2}{4}(C_B - C_0)^{-\frac{1}{2}} + \frac{1}{4\,\mu\,\pi}(C_B - C_0)^{\frac{1}{2}}\right),$$

$$\frac{dV}{dC_B} = \sqrt{\frac{\pi}{\mu}}\left(\frac{{r_p}^2}{4\sqrt{(C_B - C_0)}} + \frac{\sqrt{(C_B - C_0)}}{4\,\mu\,\pi}\right).$$

Therefore the water flow rate, change in volume per second, is,

$$Q_{H_2O}(C_B) = \frac{dV}{dt} = \sqrt{\frac{\pi}{\mu}}\left(\frac{{r_p}^2}{4\sqrt{(C_B - C_0)}} + \frac{\sqrt{(C_B - C_0)}}{4\,\mu\,\pi}\right)\frac{dC_B}{dt},$$

Where Q_{H_2O} is the flow rate of water and $\frac{dC_B}{dt}$ is the change in capacitance per second, the previously mentioned slope that is experimentally found. Therefore the water flux through the membrane is,

$$\Phi_{H_2O}(C_B) = \frac{Q_{H_2O}(C_B)}{A_m^B}.$$

Results

For **black lipid membranes** (BLM), the known conversion factor, from surface area to capacitance is ~0.5 μF/cm^2 (Bartlett 2008). Using this knowledge, we can extract the surface area for our PE: PC lipid membrane. The radius of the glass pipette we use to paint our membranes is 0.017cm, so the capacitance should be 456 pF. For our first data set we collected data for membranes that had low initial capacitances, ~150pF. The discrepancy between our actual capacitance and ideal capacitance is due to the decane torus surrounding the lipid membrane. The decane torus does not contribute significantly to capacitance because it is much thicker than the lipid bilayer; rather it acts as a reservoir of lipids that can be utilized for membrane expansion (figure 2).

Once a stable membrane is formed on a pipette tip, the temperature is cycled ±5 °C allowing the decane torus to anneal. The annealing process is observed once the membrane capacitance does not change after a 5°C cycle. Once the membrane has stabilized and the decane has annealed, the temperature is increased until the capacitance to ~180% its original capacitance (figure 4). Upon addition of the gradient, the capacitance initially decreased linearly with a slope that depended on the amount of gradient exchanged with the solution (figure 5A). Using this $\frac{dC}{dt}$, we could find the water flux in the following way.

Using this equation we found the water flux through our membrane (figure 5B). Since the flux is dependent on the difference between the concentrations of the two solutions, we can normalize the flux values we found by factoring in the affect of the difference in osmolarity. This normalization has been named the osmotic permeability of water, which is a previously found and accepted value. The osmotic permeability of water shows that the ability of water to diffuse across a membrane due to a difference

between osmotic or hydraulic pressures. The osmotic permeability of water is calculated using both the molecular weight of water and the change in osmolarity using,

$$\mathcal{P}_w = \frac{\Phi_{H_2O}(C_B)}{\Delta OsM * \mathrm{M}(H_2O)},$$

where $\mathcal{P}_w$ is the permeability of water, ΔOsM is the difference in osmolarity between the initial and the final solutions, and $\mathrm{M}(H_2O)$ is the molar mass of water (Stein 1989). The calculated osmotic permeability of water is found in figure 5C.

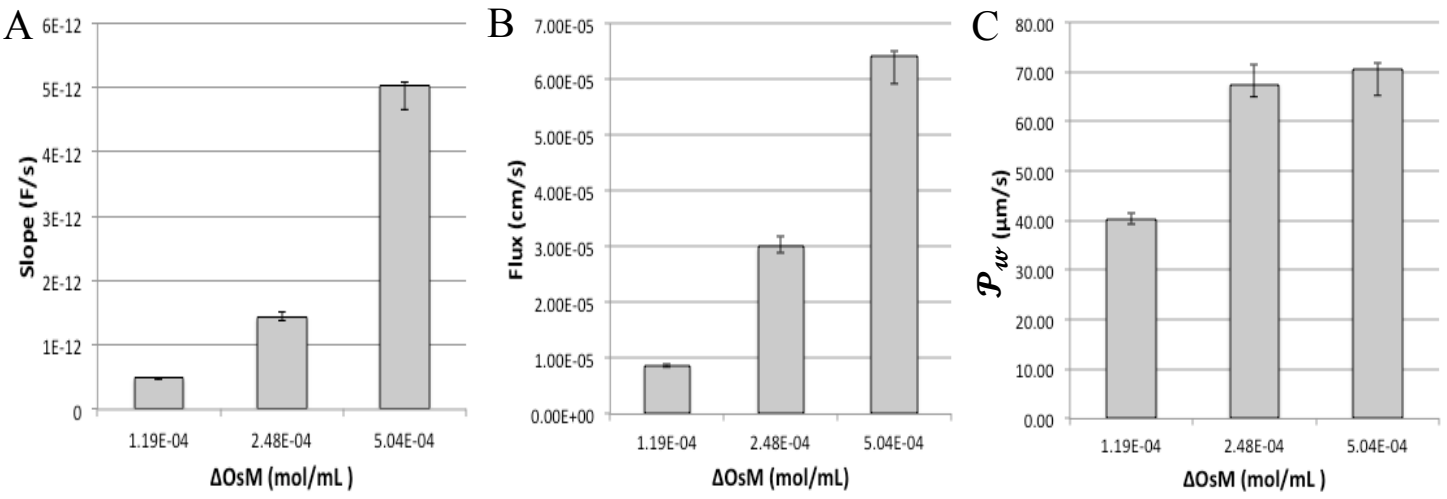

Figure 1: The three graphs represent three different experiments ran. The two higher changes in osmolarity (.25 and .5 mmol/mL) account for lower initial capacitances and the lower change in osmolarity (.12 mmol/mL) had a higher initial capacitance. Therefore the error bars account for the possible slopes that could be interpreted from the experimental data (figure 4). **A.** Change in capacitance per second as a function of change in osmolarity (amount of gradient added). **B.** This gives the flux determined as a function of change in osmolarity. **C.** Shows the permeability of water as a function of change in osmolarity.

Discussion

As mentioned before, the decane torus acts as a reservoir of lipids that provide lipids to the expanding membrane, and it also helps create a smooth surface where a membrane can be painted on the glass. However, the membrane capacitance is dependent of the size of the decane torus. If the capacitance is smaller than expected for the inner diameter of the glass pipet, then we can assume that the decane torus is large. The decane adds an interesting artifact to our experiment. We assume that it does allow the membrane to expand because it acts as a reservoir; however, its interaction with the membrane during thermal expansion is uncertain. We have hypothesized that through annealing the decane torus, we get the decane to a fixed radius no matter its temperature. We found that a membrane with the surrounding decane annealed gives a constant capacitance in its unbulged state. We assume that, although the decane is moving with the membrane during thermal expansion, the annealed decane torus' radius is constant; thus, we can assume that the only addition of volume to the spherical capacitance is due to the membrane increasing its surface area. This implies that the flux is mainly affected by what we see in the change in capacitance.

This hypothesis was confirmed by our experimental data. The initial unbulged capacitance and the $\mathcal{P}_w$ are independent of each other. We observed both high and low values for the $\mathcal{P}_w$ in low and high capacitances, implying that $\mathcal{P}_w$ does not change with different membrane surface areas. If we can get consistent values for $\mathcal{P}_w$ then we know that the water flux through a membrane is also independent of the size of the decane torus. Therefore, as shown in figure 6B, different values of $\mathcal{P}_w$ are the same for both high and low decane surface areas. The values that we found are in the accepted values for $\mathcal{P}_w$, which range from 1-500μm/s (Weiss 1996).

Jansen noted that the permeability of water depended on the temperature. They measured $\mathcal{P}_w$ at two fixed temperatures, 20°C and 70°C. In some lipids, it changed by 3 orders of magnitude. (Jansen 1995). To avoid possible problems with temperature affects, we kept the temperature constant as the gradient was applied, typically between 35-40°C. Therefore, the possible concern of $\mathcal{P}_w$ changing with temperature should not have significant affects on our values.

In conclusion, this method provides another way of measuring the water flux through a lipid membrane, since we found results that were in line with the accepted permeability of water values (Weiss 1996). We also came to the conclusion that the decane torus does not seriously affects the permeability of water; rather, the two are unrelated. Relevant to our lab, we have concluded that a fusion rate experiment is not possible since the solutions equilibrate too quickly.

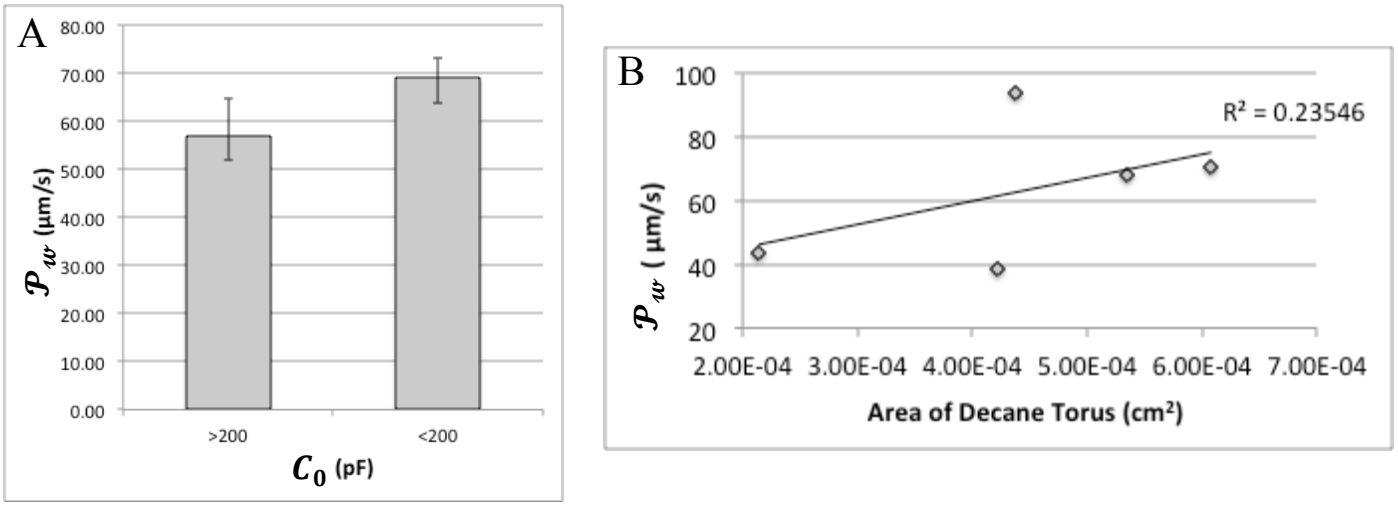

Figure 6: A. Permeability of water as a function of initial capacitance. Note how the initial capacitance does not significantly correlate with the permeability of water. **B.** Shows the permeability of water as a function of the area of the decane torus. This further confirms that the amount of decane in a membrane isn't directly correlated to the permeability of water.

Acknowledgements

I would like to thank my wife for her support in all aspects of my life, both school and home. I would like to thank my professor and mentor, Dr. Dixon J. Woodbury for the countless hours of helping and advising me in this project. His knowledge of lipid membranes helped to conceptualize how a membrane might behave in different situations. I would like to also thank Landon Goggins for his collaboration and help with both the experiments and analyzing the data for this project.

Appendix A: Derivation of Spherical Cap Volume

Using the figure to the right, we can see the circumference of the disk making the spherical cap to be,

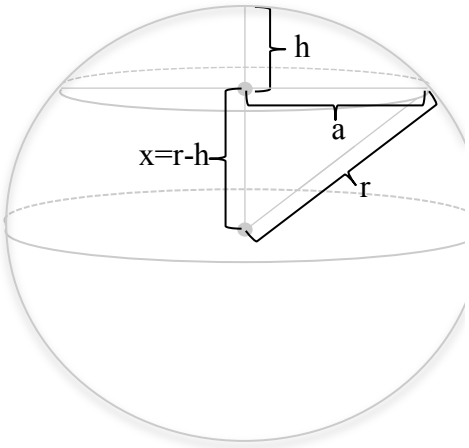

$$C = 2\pi a,$$

with the radius of the spherical cap, a, being,

$$a = \sqrt{r^2 - x^2}.$$

Therefore the surface area is,

$$A = \int_0^h C\, ds,$$

$$A = \int_0^h 2\pi\sqrt{r^2 - x^2}\, ds.$$

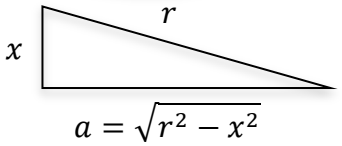

Since as we integrate we change in both x and y ds can be found using figures below to be

$$ds = \sqrt{dy^2 + dx^2},$$

$$ds = dx\sqrt{\left(\frac{dy}{dx}\right)^2 + 1},$$

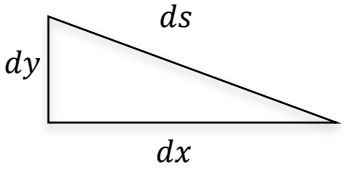

with the slope being

$$\frac{dy}{dx} = \frac{x}{\sqrt{r^2 - x^2}},$$

$$ds = dx\sqrt{\left(\frac{x}{\sqrt{r^2 - x^2}}\right)^2 + 1} = \sqrt{\frac{x^2}{r^2 - x^2} + \frac{r^2 - x^2}{r^2 - x^2}}\, dx,$$

$$ds = \frac{r}{\sqrt{r^2 - x^2}}\, dx$$

Therefore continuing our integral from before for the surface area, we find,

$$A = \int_0^h 2\pi\sqrt{r^2 - x^2}\left(\frac{r}{\sqrt{r^2 - x^2}}\,dx\right),$$

$$A = \int_0^h 2\pi r\,dx = 2\pi r x\Big|_0^h,$$

$$A = 2\pi r h.$$

Then we can find the radius in terms of the height and radius of the spherical cap, a, is,

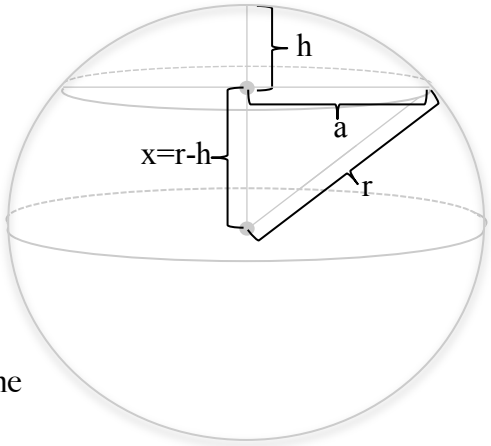

$$r^2 = x^2 + a^2 = (r - h)^2 + a^2,$$

$$r^2 = (r^2 - 2rh + h^2) + a^2,$$

$$2rh = h^2 + a^2,$$

$$r(h, a) = \frac{h^2 + a^2}{2h}.$$

Finally, we can find the volume by integrating vertically over one half the surface area.

$$V = \frac{1}{2}\int_0^h A\,dx,$$

$$V = \frac{1}{2}\int_0^h 2\pi r x\,dx,$$

$$V = \pi\int_0^h \left(\frac{x^2 + a^2}{2x}\right)x\,dx,$$

$$V = \frac{\pi}{2}\int_0^h x^2 + a^2\,dx = \frac{\pi}{2}\left(\frac{x^3}{3} + xa^2\right)\Big|_0^h,$$

$$V = \frac{\pi}{2}\left(\frac{h^3}{3} + ha^2\right),$$

$$V = \frac{\pi h}{6}(3a^2 + h^2).$$

■

Appendix B: Glossary

1. **Black Lipid Membranes** (BLM)- "free-hanging bilayers over micrometer sized aperture in thin hydrophobic substrate and are only held by the lateral tension between the lipids." (Atanasova 2007)
2. **Capillary action** –The ability for a solution to flow against gravity using inter-molecular forces between the surface and the solution. For our experiment, the water fills glass capillary pipette because there is strong inter-molecular interaction between the glass and water.
3. **Electrophysiology** – The study of the human body using electrical principles such as capacitance, voltage, and current. For our study, we measured the capacitance and current across a lipid bilayer, providing insight to the membranes surface area.
4. **Exocytosis** – This is the cellular process that involves the release of material from inside a cell to outside the cell. For example, a vesicle, inside the cell, releases neurotransmitter outside the cell through exocytosis.
5. **Fusion** – Fusion is the joining of the cell membrane and secretory vesicle in the process of exocytosis.
6. **SNARE proteins** – A three-protein complex that aids the process of exocytosis in the human body. We did not use SNARE proteins in our experiment, but rather we used a concentration gradient to drive vesicle fusion.

Appendix C: References

Background. (2008). *National Institute of Drug Abuse*. Retrieved April 5, 2012, from http://m.drugabuse.gov/publications/brain-power/grades-2-3/sending-receiving-messages-module-3/background.

Bartlett, P. N. (2008). *Bioelectrochemistry: Fundamentals, experimental techniques and applications* John Wiley \& Sons.

Bock, L. V., B. Hutchings, H. Grubmuller, and D. J. Woodbury. (2010). Chemomechanical regulation of SNARE proteins studied with molecular dynamics simulations. *Biophys J* 99:1221-1230.

Haines, H. T. (1994). Water transport across biological membranes. *FEBS Letters 346, 115-122.*

Holz, R., & Finkelstein, A. (1970). The water and nonelectrolyte permeability induced in thin lipid membranes by the polyene antibiotics nystatin and amphotericin B. *The Journal of General Physiology*, *56*, 125.

Jansen, M., & Blume, A. (1995). A comparative study of diffusive and osmotic water permeation across bilayers composed of phospholipids with different head groups and fatty acyl chains. *Biophysical Journal*, *68*, 997-1008.

Lang, T., N. D. Halemani, and B. Rammner. (2008). Interplay between lipids and the proteinaceous membrane fusion machinery. *Progress in Lipid Research* 47:461-469.

Neuron. (2012). *In Encyclopædia Britannica*. Retrieved March 24, 2012, from from http://www.britannica.com/EBchecked/topic/410669/neuron.

Reviakine, I., & Brisson, A. (2000). Formation of supported phospholipid bilayers from unilamellar vesicles investigated by atomic force microscopy. *LANGMUIR*, *16*, 1806-1815.

Stein, W.D. (1989). Kinetics of transport: Analyzing, testing, and characterizing models using kinetic approaches. In Fleischer, S. and Fleischer, B., eds., *Methods in Enzymology*, vol. 171, *Biomembranes*, pt. R, *Transport theory: Cells and Model Membranes*. Academic Press, New York.

Tenchov, B. G., Petsev, D. N., Koynova, R. D., Vassilieff, C. S., Meyer, H. W., & Wunderlich, J. (1989). Liposome—glass interaction. Influence of the lipid bilayer phase state. *Colloids and Surfaces*, *39*(2), 361-370. doi: 10.1016/0166-6622(89)80286-0

Weiss, T. F. (1996). *Cellular biophysics: Transport.* (Volume 1). MIT Press.

Wiederhold, K., & Fasshauer, D. (2009). Is assembly of the SNARE complex enough to fuel membrane fusion? *Journal of Biological Chemistry*, 284(19), 13143-13152.

Woodbury, D. J., & Hall, J. E. (1988). Role of channels in the fusion of vesicles with a planar bilayer. *Biophysical Journal*, 54(6) , 1053-1063. doi: 10.1016/S0006-3495(88)83042-X